



INFLUENCE OF LONGITUDINAL REINFORCEMENT LAYOUTS ON RC WALL PERFORMANCE

Angelica ROSSO¹, João ALMEIDA², Raluca CONSTANTIN³, Katrin BEYER⁴, Sri
SRITHARAN⁵

ABSTRACT

Design recommendations for longitudinal reinforcement layouts of reinforced concrete (RC) walls have been derived from plane section analyses. Such an analysis generally favours wall layouts with boundary elements containing large amounts of vertical reinforcement, providing higher moment resistance and larger ductility capacity than the same reinforcement distributed evenly along the wall length. The main disadvantage of a design method based on a plane section analysis is that it disregards the beneficial influence that the distribution of longitudinal reinforcement has on the member shear performance and reduction of crack widths. In order to better understand the seismic performance of RC walls with concentrated and distributed longitudinal reinforcement layouts, this paper starts with a review of simple mechanical models and code prescriptions on stability of rectangular walls, sliding shear resistance, and required confinement reinforcement. The relevant expressions from this survey are then applied to a case study comprising two walls. In addition, the latter are numerically simulated with an advanced nonlinear membrane model to avoid the limitations of plane section hypothesis. Pushover analyses show that distributed reinforcement layouts can lead to an improved wall behaviour in terms of crack widths and spacing along the wall height, as well as a different failure mechanism due to crushing of the compressed zone instead of a premature sliding shear failure at the base of the wall.

INTRODUCTION

Structural wall damages during the 2011 Christchurch earthquake showed that modern reinforced concrete (RC) walls did not respond in a ductile manner as much as expected (Sritharan et al., 2014). One observed failure mode of well-designed concrete walls with boundary elements is

¹ PhD candidate, Earthquake Engineering and Structural Dynamics Laboratory (EESD), School of Architectural, Civil and Environmental Engineering (ENAC), École Polytechnique Fédérale de Lausanne (EPFL), angelica.rosso@epfl.ch

² Post-doctoral Researcher, Earthquake Engineering and Structural Dynamics Laboratory (EESD), School of Architectural, Civil and Environmental Engineering (ENAC), École Polytechnique Fédérale de Lausanne (EPFL), joao.almeida@epfl.ch

³ PhD candidate, Earthquake Engineering and Structural Dynamics Laboratory (EESD), School of Architectural, Civil and Environmental Engineering (ENAC), École Polytechnique Fédérale de Lausanne (EPFL), raluca.constantin@epfl.ch

⁴ Assistant Professor, Earthquake Engineering and Structural Dynamics Laboratory (EESD), School of Architectural, Civil and Environmental Engineering (ENAC), École Polytechnique Fédérale de Lausanne (EPFL), katrin.beyer@epfl.ch

⁵ Professor, Iowa State University, Ames, IA 50010, USA, sri@iastate.edu

seemingly linked to an initial crushing of the wall web region adjacent to the boundary elements. The region is typically detailed with light longitudinal reinforcement and no confinement reinforcement. Since the longitudinal reinforcement concentrates in heavily confined boundary elements, these regions in the walls exhibited less damage than the web. The lack of confinement and the potential for compression strain to exceed larger values outside the boundary elements make the webs to experience crushing of both the cover and core concrete. Similar damage patterns for walls with such concentrated reinforcement layouts were observed in laboratory tests (e.g., Beyer et al., 2008; Brueggen 2009). As an alternative to concentrated reinforcement layouts, the longitudinal reinforcement can be distributed evenly along the wall length, which has been shown to produce better seismic performance (Priestley, 2003). Sections with distributed reinforcement have larger yield curvatures and compression zone depths; hence, if concrete crushing becomes critical, the ultimate curvature might be smaller than for layouts with strong boundary elements, which reduces the curvature ductility capacity. These considerations suggest the need to investigate the best wall longitudinal reinforcement layout for optimum seismic performance.

Focussing on RC cantilever walls (length l_w , width b_w , and height h_w , see Figure 1a) with a constant axial load, this paper investigates the effect of different longitudinal reinforcement layouts on lateral load performance with respect to several issues. First, potential failures by out-of-plane buckling and shear sliding are investigated, and then the required confining reinforcement and the length of the confined regions are examined. Finally, two different longitudinal reinforcement configurations are analysed by means of nonlinear shell element models using program VecTor2 (Wong and Vecchio, 2013) to see the impact of the reinforcement distribution on the wall response.

OUT-OF-PLANE BUCKLING

Mechanics of out-of-plane buckling of RC walls

The lateral stability of ductile RC walls subjected to in-plane seismic loading is usually investigated by idealizing the plastic hinge regions in the wall edges as an axially loaded column under large amplitude cyclic tension and compression. To date, there are few indications on how to estimate or define the wall region that undergoes out-of-plane buckling—represented in Figure 1a by $l_b \times h_b$ —and how the latter relates to the longitudinal reinforcement layout, in particular the presence of confined boundary elements.

The mechanics of out-of-plane buckling can be summarised as follows, for a wall with double layer reinforcement. At large in-plane curvature demands, the wall edge region develops large tensile strains that cause wide near-horizontal cracks across the width of the section. That leads to longitudinal reinforcement yielding in tension and eventual strain-hardening. Upon unloading, an elastic strain recovery takes place, although the cracks remain wide due to the plastic tensile strains previously accumulated in the rebars. During reloading in compression, and until crack closure, the compression force must be resisted solely by the two layers of vertical reinforcement. This stage is typically accompanied by an incipient out-of-plane displacement, which occurs due to an unavoidable eccentricity of the axial force C acting in this region (see Figure 1b), and construction misalignments in the position of the longitudinal reinforcements. While the rebars retain their significant axial stiffness before yielding in compression, the out-of-plane displacement tends to remain small. However, as compression increases the longitudinal rebar near the concave side will yield, originating an abrupt reduction in stiffness and a consequent increase in the out-of-plane displacement. It is noted that, at this point, the second layer of longitudinal reinforcement—which has not yet yielded in compression—is the main source of out-of-plane stiffness. Depending on the magnitude of the tensile strain previously attained (i.e., before unloading), different scenarios can then take place as compression progresses. The cracks may close, re-establishing compressive concrete contact, or they may remain open leading to compression yielding of the second layer of reinforcement. In the latter case, out-of-plane displacements will abruptly increase, leading to wall buckling failure. Intermediate conditions, wherein the second layer of reinforcement yields but cracks still close, at least partially, are also possible. Independently of the scenario that effectively takes place, the occurrence of out-of-plane

displacements and second-order moments will affect the in-plane wall response and should therefore be taken into account.

In view of the above description, it is unsurprising that past studies (Paulay and Priestley, 1993; Chai and Kunnath, 2005) have identified the critical parameter governing the wall stability as the maximum tensile strain imposed on the vertical wall edge regions. In what could appear at first glance as somewhat counter-intuitive, the maximum experienced compressive strain plays a comparatively minor role. The next section briefly recalls available models to estimate the maximum tensile strain that may be imposed on a RC column while ensuring its lateral stability. It is noted that the column length l_0 , which corresponds to the distance between points of contraflexure in the buckled wall (see Figure 1a), appears to require future research. Nevertheless, Paulay and Priestley (1993) suggest that, as large strains may be expected only over the lower part of the plastic region, l_0 can be taken as equal to a proposed formula for the equivalent plastic hinge length.

Models to estimate maximum tensile strain

Consider Figure 1b, which depicts the internal forces at midheight of the buckling length l_0 where the out-of-plane displacement $\delta = \xi b_w$ is larger. The total compression force C is taken by both the steel compression force C_S and the concrete compression force C_C , whose resultant is at an eccentricity γb_w . Vertical force and moment equilibrium produce:

$$C = C_C + C_S \quad (1)$$

$$C_C = \frac{\xi}{\gamma} \cdot C \quad (2)$$

Assuming an equivalent rectangular compression stress block for the concrete compression force, and that the steel has reached its yield strength, one can rewrite C_C and C_S as:

$$C_C = 2b_w \cdot \left(\frac{l}{2} - \gamma\right) 0.85f_c \quad (3)$$

$$C_S = \rho_b b_w f_y \quad (4)$$

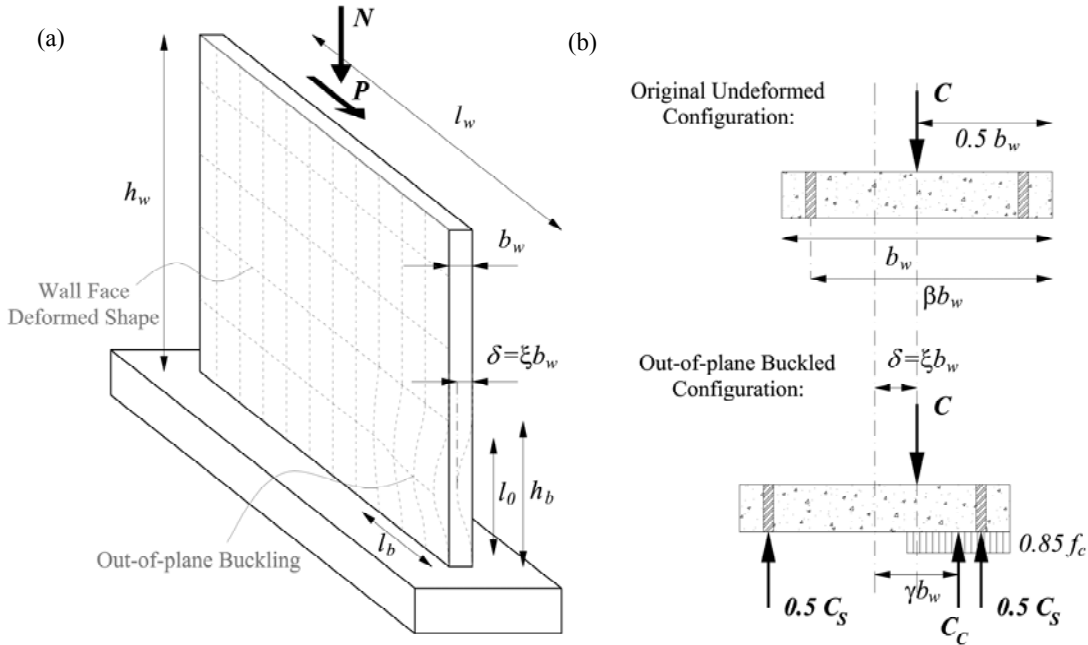


Figure 1. (a) Geometrical characteristics of the wall and out-of-plane buckling; (b) Equilibrium of external and internal forces at midheight of buckling region (adapted from Paulay and Priestley, 1993).

Substituting Eq. (3) and Eq. (4) into Eq. (1) and Eq. (2), one obtains:

$$\gamma = \frac{1}{2} \left[(\xi + 0.5) + \sqrt{(\xi + 0.5)^2 - 2\xi \cdot (1 + 1.176m)} \right] \quad (5)$$

where $m = \rho_b f_y / f_c$ is the mechanical reinforcement ratio of the wall strip. This equation has real solutions only when the term inside the square root is non-negative:

$$\xi \leq \xi_c = 0.5 \cdot \left(1 + 2.35m - \sqrt{5.53m^2 + 4.70m} \right) \quad (6)$$

The previous equation represents the stability criterion of RC walls as derived by Paulay and Priestley (1993). The upper limit ξ_c represents the critical normalized out-of-plane displacement that marks the onset of wall instability.

The increase in arc length due to wall out-of-plane displacement results from the axial elongation of the wall strip over the buckling length l_0 . Based on this assumption, Paulay and Priestley (1993) and Chai and Elayer (1999) established the following two relationships between the maximum average axial tensile strain over l_0 and the normalized out-of-plane displacement ξ_c , respectively:

$$\varepsilon_{sm,c} = 8\beta \left(\frac{b_w}{l_0} \right)^2 \xi_c \quad (7)$$

$$\varepsilon_{sm,c} = \frac{\pi^2}{2} \left(\frac{b_w}{l_0} \right)^2 \xi_c + 3\varepsilon_y \quad (8)$$

According to both studies, l_0 may be taken as the equivalent plastic hinge length $l_p = 0.20 \cdot l_w + 0.044 \cdot h_w$. Paulay and Priestley (1993) derived Eq.(7) from geometrical considerations. The parameter β takes into account the position of the vertical reinforcement within the wall thickness, as depicted in Figure 1b (for walls with a single layer of vertical reinforcement $\beta=0.5$). Eq.(8), developed by Chai and Elayer (1999), is a phenomenological equation based on tests of axially loaded concrete columns reinforced with two layers of vertical bars under large strains amplitudes. Therein, ε_y is the yield strain of the reinforcement. This approach ignores the reduced out-of-plane stability expected for walls with a single layer reinforcement layout.

Eq. (7) and Eq. (8) can be rewritten as explicit functions of the reinforcement ratio:

$$\varepsilon_{sm,c} = 8\beta \left(\frac{b_w}{l_0} \right)^2 \cdot 0.5 \cdot \left[1 + 2.35 \frac{\rho_b f_y}{f_c} - \sqrt{5.53 \left(\frac{\rho_b f_y}{f_c} \right)^2 + 4.70 \left(\frac{\rho_b f_y}{f_c} \right)} \right] \quad (9)$$

$$\varepsilon_{sm,c} = \frac{\pi^2}{2} \left(\frac{b_w}{l_0} \right)^2 \cdot 0.5 \cdot \left[1 + 2.35 \frac{\rho_b f_y}{f_c} - \sqrt{5.53 \left(\frac{\rho_b f_y}{f_c} \right)^2 + 4.70 \left(\frac{\rho_b f_y}{f_c} \right)} \right] + 3\varepsilon_y \quad (10)$$

The equations above should provide conservative predictions of a tensile strain below which crack closure, and subsequent crushing limit state, can be reached. The application example in the last section of the current paper will illustrate the use of these expressions and the conclusions that can be obtained.

SLIDING SHEAR FAILURE

Several cyclic RC wall tests (e.g., Paulay et al., 1982; Salonikios et al., 2000) have shown that after a few reversed cyclic loads that cause significant yielding in the flexural longitudinal reinforcement, wall sliding can occur at flexural cracks that form along the entire wall length. These cracks are approximately horizontal and develop through interconnection of several cracks. Such

sliding of walls causes a significant reduction in lateral stiffness, particularly at low load intensities, a reduction in energy dissipation, and a premature sliding shear failure (Paulay et al., 1982). This failure mode is more common in walls with a low reinforcement ratio and smaller diameter bars in the web (Preti and Giuriani, 2011). In order to avoid sliding failure, the longitudinal reinforcement may be distributed (Priestley, 2003).

To prevent shear sliding, in design $V_{Ed} \leq V_{Rd,S}$ is ensured at potential failure planes, where V_{Ed} is the shear demand and $V_{Rd,S}$ is the sliding shear resistance. In the following, the sliding shear resistance according to three different design standards are reviewed and evaluated for both concentrated and distributed longitudinal reinforcement layouts.

Sliding shear resistance according to Eurocode 8

According to Eurocode 8 (CEN, 2004), the shear resistance is defined as the sum of dowel resistance of vertical bars V_{dd} , shear resistance of inclined bars V_{id} , and friction resistance V_{fd} :

$$V_{Rd,S} = V_{dd} + V_{id} + V_{fd} \quad (11)$$

with:

$$V_{dd} = \min \left\{ \begin{array}{l} 1.3 \cdot \sum A_{sj} \cdot \sqrt{f_c f_y} \\ 0.25 \cdot f_y \cdot \sum A_{sj} \end{array} \right. \quad (12)$$

$$V_{id} = \sum A_{sj} \cdot f_y \cdot \cos \varphi \quad (13)$$

$$V_{fd} = \min \left\{ \begin{array}{l} \mu_f \cdot \left[\left(\sum A_{sj} \cdot f_y + N_{Ed} \right) \cdot \frac{x_u}{l_w} + \frac{M_{Ed}}{z} \right] \\ 0.5 \cdot \eta \cdot f_c \cdot x_u \cdot b_w \end{array} \right. \quad (14)$$

where μ_f is the concrete-to-concrete friction coefficient, z is the internal lever arm of the tension and compression force resultant in the wall which can be assumed equal to $0.8l_w$, x_u is the neutral axis depth, φ is the angle between shear-friction reinforcement and shear plane, $\sum A_{sj}$ is the sum of the area of the vertical bars within the web, $\sum A_{si}$ is the sum of the area of all inclined bars within the web, and $\eta = 0.6 \cdot (1 - f_c/250)$.

Sliding shear resistance according to ACI Code

ACI Code (ACI Committee 318, 2011) computes the sliding shear resistance based on a friction mechanism, but without accounting for the dowel action of the longitudinal bars. The sliding shear resistance of shear-friction reinforcement perpendicular or inclined to the shear plane respectively is computed as:

$$V_{Rd,S} = A_{vf} f_y \mu_f \quad (17)$$

$$V_{Rd,S} = A_{vf} f_y \cdot (\mu_f \sin \varphi + \cos \varphi) \quad (18)$$

where μ_f is the coefficient of friction and A_{vf} is the total area of shear-friction reinforcement, intended as the sum of all bars crossing the section in which the sliding shear resistance is checked. Note that ACI 318 does not explicitly account for the contribution of the axial force to the sliding shear resistance. In fact, it is specified in the commentary section that the friction resistance due to a compression force acting across a shear plane can be taken into account, provided that it is certain that this compressive force is permanent.

Sliding shear resistance according to NZS 3101

According to the New Zealand Standard on Concrete Structures (New Zealand Standard, 2006), the nominal shear strength results from a friction resistance, but, unlike ACI 318, it accounts for the friction resistance resulting from the axial load N_{Ed} . The sliding shear resistance $V_{Rd,S}$ is therefore computed for shear-friction reinforcement perpendicular or inclined to the shear plane respectively as:

$$V_{Rd,S} = (A_v f_y + N_{Ed}) \mu_f \quad (19)$$

$$V_{Rd,S} = A_v f_y (\mu_f \sin \phi + \cos \phi) + N_{Ed} \mu_f \quad (20)$$

Influence of reinforcement layout on sliding shear failure

According to the equations presented above, ACI 318 and NZS 3101 establish a direct proportional relation between the sliding shear strength and the reinforcement crossing the potential sliding shear plane. Since for the same moment demand, the choice of a distributed reinforcement layout leads to a slightly higher total longitudinal reinforcement ratio than a concentrated reinforcement layout, the distributed reinforcement layout leads to a slightly higher sliding shear resistance than the concentrated reinforcement layout.

In Eurocode 8, the proposed relation to compute the sliding shear strength is more complex. Considering a simple reinforcement layout, without inclined bars or additional bars arranged specifically for resisting sliding, the reinforcement content within the web influences the predicted sliding shear resistance as follows:

- The choice between distributed or concentrated layout strongly influences the reinforcement content of the web and therefore the value of $\sum A_{sj}$ in Eq. (12) and Eq. (13). Since only the web reinforcement is considered when computing the dowel resistance, distributed reinforcement layouts lead to larger dowel resistance against sliding.
- The increase of the reinforcement ratio in the web causes a larger neutral axis depth. The contribution of friction resistance is directly proportional to the neutral axis depth as shown in Eq.(15). Hence, Eq.(16), is higher for distributed reinforcement layouts than for concentrated reinforcement layouts.

The case-study of the last section shows a comparison between the sliding resistance computed for a specific wall according to the three codes.

DETAILING FOR LOCAL DUCTILITY

In RC walls, the concrete cover is usually allowed to exceed its ultimate strain capacity and spall. The required curvature ductility capacity μ_ϕ for the walls to sustain an earthquake load, therefore depends on the strain capacity of the confined concrete. The length of the confined zone is a function of the neutral axis depth x_u . This length can be computed by fibre analysis or by simple equilibrium considerations of the critical section. Since the confinement reinforcement is provided to avoid crushing of extreme concrete fibres in the confined core until after both the longitudinal reinforcement bars in tension and compression yielded, the latter results in the following approximation for x_u (Fardis, 2009):

$$x_u \approx \frac{v + \omega_v}{\left(1 - \frac{\varepsilon_{co}^*}{3\varepsilon_{cu}^*}\right) \frac{f_c^*}{f_c} \frac{b_o h_o}{b_c h_c} + 2\omega_v} l_w \quad (21)$$

where $\omega_v = A_{sv} f_y / h_c b_c f_c$ is the mechanical reinforcement ratio of the vertical bars in the unspalled section, h_c and b_c are, respectively, the depth and width of the original unspalled concrete section, h_o and b_o are the corresponding dimensions of the confined core, f_c and f_c^* are the ultimate concrete compression strength in the unspalled section and in the concrete core, respectively, ε_{co}^* and ε_{cu}^* are the concrete strains at the peak stress in compression and the compressive strain at which spalling is expected.

Eq. (21) shows that the variation of reinforcement layout affects the neutral axis depth and that it increases with increasing web reinforcement ratio ω_v . In the following section, different design standards are examined with regard to the provisions for the minimum confinement length and its dependence on the reinforcement layout.

Length of confined zones according to Eurocode 8

According to Eurocode 8 (CEN, 2004), the length of the confined zone may be limited to a distance from the hoop centerline near the extreme compression fibre equal to:

$$l_c \geq x_u \left(1 - \frac{\varepsilon_{cu2}}{\varepsilon_{cu2,c}} \right) \quad (22)$$

where ε_{cu2} , the compressive strain at which spalling is expected, may be taken as being equal to 0.0035 and $\varepsilon_{cu2,c}$, the ultimate strain of confined concrete, is estimated on the basis of EN 1992-1-1:2004 as $\varepsilon_{cu2,c} = 0.0035 + 0.1\alpha\omega_{wd}$. In addition, the length of the confined zone should not be less than of $0.15l_w$ and $1.50b_w$.

Length of confined zones according to ACI 318

According to ACI 318 (ACI Committee 318, 2011), if the neutral axis depth x_u exceeds the limit value c_c , the extreme fiber compression strain exceeds the limiting strain $\varepsilon_{cu2} = 0.003$. As a result, special confined detailing is required:

$$c_c = \frac{l_w}{600(\delta_u/h_w)} \quad (23)$$

where the design drift, δ_u/h_w , shall not be taken less than 0.7%. The length of these zones shall extend horizontally from the extreme compression fibre as follows:

$$l_c \geq \max(x_u - 0.1 \cdot l_w; 0.5x_u) \quad (24)$$

where $x_u - 0.1 \cdot l_w$ is based on Eq.(23) assuming a design drift of 1.5%.

Length of confined zones according to New Zealand Standard

According to the New Zealand Standard on Concrete Structures NZS 3101 (New Zealand Standard, 2006), when the neutral axis depth at the ultimate limit state exceeds the limit value c_c , special boundary elements should be designed. The value of c_c is determined as follows:

$$c_c = \frac{0.1\phi_{ow}l_w}{\lambda} \quad (25)$$

where ϕ_{ow} is the ratio of moment resistance at overstrength to the design moment resulting from earthquake actions (both moments are obtained at the base section of a wall), and λ is assumed to be 1 for limited ductile regions and 2 for ductile plastic regions. The length of the confined region of the compressed wall section is then determined using Eq. 26.

$$l_c \geq \max(x_u - 0.7c_c; 0.5x_u) \quad (26)$$

Influence of reinforcement layout on the length of confined zones

For all three design documents considered in this study, the minimum required confinement length is longer in case of the distributed layout, given that the neutral axis depth is larger when the web reinforcement ratio ρ_v increases, as seen in Eq. (21). When comparing the required length of confined zones, Eurocode 8 produce the highest and ACI 318 demand the least values for l_c .

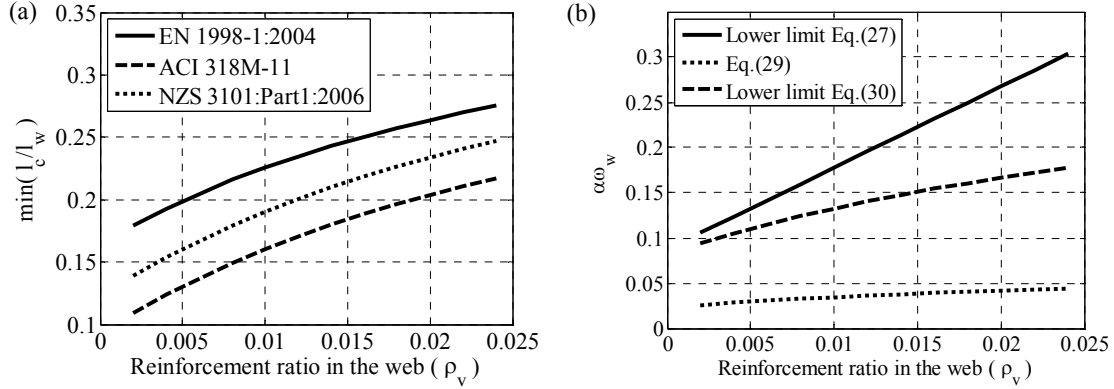


Figure 2. (a) Comparison of the minimum required horizontal length of the confined zone normalized with respect to the total length as a function of the reinforcement ratio in the web, and (b) minimum content of confining reinforcement as a function of the reinforcement ratio in the web.

Confining reinforcement content according to Eurocode 8

Eurocode 8 requires that a minimum value of curvature ductility capacity, μ_ϕ , should be ensured at the critical regions of walls. Unless a more precise method is used, this value may be accomplished by means of confining reinforcement within edge regions of the cross-section.

To determine the amount of confining reinforcement in rectangular walls, the mechanical volumetric ratio $\omega_{wd} \geq \left(\frac{\text{Volume of confining hoops}}{\text{Volume of concrete core}} \right) f_{yd}/f_{cd}$ in confined zones should satisfy the following expression:

$$\omega_{wd} \geq \frac{1}{\alpha} 30 \mu_\phi (v_d + \omega_v) \varepsilon_{sy,d} \frac{b_c}{b_o} - 0.035 \quad (27)$$

where v_d is the normalized design axial force, $\varepsilon_{sy,d}$ is the design value of tension steel strain at yield, and α is the confinement effectiveness factor. This equation was derived from curvature ductility demand $\mu_\phi = \phi_u/\phi_y$, assuming $\phi_y = \lambda \varepsilon_y/h_c$ ($\lambda=1.44$ for walls) and $\phi_{cu} = \varepsilon_{cu}^*/\xi_{cu}^* h_0$ (Fardis, 2009), with

$$\varepsilon_{cu}^* = \lambda \mu_\phi \varepsilon_y \xi_{cu}^* \frac{h_o}{h_c} \quad (28)$$

The assumptions adopted from Eq. (28) to reach Eq.(27) lead to very high values for ω_w in case of distributed reinforcement layouts (Figure 2b). These values are difficult to adopt in real designs. These excessive confinement reinforcement ratios are due to the approximations introduced to obtain ω_{wd} in a simplified manner.

The equation for the required confinement reinforcement ratio, which is obtained from equilibrium considerations is as follows:

$$\omega_w = \frac{1}{\alpha} \frac{(v + \omega_v) \lambda \mu_\phi \varepsilon_y + \frac{\varepsilon_{cu}^* f_c^* b_o}{3 f_c b_c}}{0.1 \cdot \left(\frac{f_c^* b_o}{f_c b_c} + 2 \omega_v \frac{h_c}{h_o} \right)} - 0.035 \quad (29)$$

Starting from the above equation and making assumptions similar to the ones adopted to reach the Eurocode 8 relation except for maintaining the mechanical reinforcement ratio in the denominator, the following expression can be derived:

$$\omega_{wd} \geq \frac{I}{\alpha} \cdot \frac{I}{0.1 + 0.2\omega_v} \left[2.88\mu_\phi (v_d + \omega_v) \varepsilon_{sy,d} \frac{b_c}{b_o} \right] - 0.035 \quad (30)$$

For a concentrated reinforcement layout the denominator tends to be 0.1 since $0.2\omega_v$ is negligible when compared to 0.1 , and therefore Eq. (30) leads to Eq. (27) which is reported in Eurocode 8.

Figure 2b shows that the lower limit of Eq. (27), proposed in the Eurocode 8, leads to a confining reinforcement content that is higher than the one needed to satisfy equilibrium (Eq. (29)). The Eq. (30) proposed here, still providing precautionary values, follows better the trend of the curve which represent real equilibrium and moreover for a concentrated layout (left side of the plot) provides values of confining reinforcement content close to the ones computed using Eurocode 8, while for a distributed layout (right side of the plot) provides more reasonable values that lead to feasible layouts of confining reinforcement.

Confining reinforcement content according to ACI Code

According to ACI Code (ACI Committee 318, 2011) the total cross-sectional area of rectangular hoop reinforcement should satisfy the following expression:

$$A_{wd} = \min \left\{ 0.3 \frac{s_h b_w f_c}{f_y} \left(\frac{A_g}{A_c} - 1 \right); 0.09 \frac{s_h b_w f_c}{f_y} \right\} \quad (31)$$

where s_h is horizontal spacing of hoops, A_g and A_c are, respectively, the areas of the total confined zone and the concrete core. These two areas implicitly depend on the neutral axis depth, since are a function of the latter the length of the confined zone, and thus of the concrete core (Eq. (24)).

Confining reinforcement content according to NZS 3101

According to NZS 3101 (New Zealand Standard, 2006) the total cross-sectional area of rectangular hoop reinforcement in the compression zone should satisfy the expression in Eq. 32:

$$A_{wd} = \alpha s_h b_o \frac{A_g f_c}{A_c f_y} \left(\frac{x_u}{l_w} - 0.07 \right) \quad (32)$$

where α is assumed to be 0.25 for limited ductile regions and 0.175 for ductile plastic regions as defined by 2.6.1.3 in this Standard.

Influence of reinforcement layout on confining reinforcement content

The relations proposed to compute the confining reinforcement content in the end regions noticeably differ between. Furthermore, as found for Eurocode 8, they may not be suitable for distributed reinforcement layouts. Their close dependence on the neutral axis depth permits, however, indicate a general trend.

In NZS 3101, the confining reinforcement content depends explicitly on the neutral axis depth, and implicitly on areas A_g and A_c , as in ACI 318. In Eurocode 8, or in the modified equations illustrated above, the reinforcement content is derived from the general neutral axis definition. Therefore, since as seen in Eq.(21), the variation of reinforcement layout affects the neutral axis depth, which increases with the increasing reinforcement ratio ρ_v ; in case of distributed layout a higher value of confining reinforcement is always required.

RC WALL WITH CONCENTRATED AND DISTRIBUTED REINFORCEMENT LAYOUTS

To illustrate some of the points discussed thus far, as well as further influence of reinforcement distribution on wall response, a slender RC wall ($h_w = 11.430$ m, $l_w = 4.570$ m and $b_w = 0.305$ m) is studied.

Firstly, its vulnerability to out-of-plane buckling is assessed with Eq.(9) and Eq. (10). Considering $f_y=455\text{MPa}$, $f_c=41.4\text{MPa}$, and $\beta=0.8$, Figure 3a shows that increasing the reinforcement ratio ρ_b reduces the maximum tensile strain corresponding to onset of wall buckling. This observation can be directly used to understand the influence of reinforcement distribution on the susceptibility to out-of-plane failure of walls. Since the critical zone in which out-of-plane instability occurs is confined to the wall boundary zone, a concentrated reinforcement layout will more adversely affect the response of the wall against out-of-plane instability than a distributed rebar detailing.

Secondly, the sliding shear resistance according to the three codes is computed. Figure 3b, which shows the comparison as a function of the total reinforcement ratio, indicates that the sliding shear strength increases at a similar rate. While the Eurocode 8 and ACI 318 lead to similar values of sliding shear strength, NZS 3101 produce much larger estimates since it accounts for the beneficial effect of the axial load. For the analysed example, the friction resistance according to Eurocode 8 was governed by Eq. (16), which only indirectly depends on the axial load (via the size of the compression zone).

Finally, the entire wall was modelled with nonlinear shell elements available in the software VecTor2 (Wong and Vecchio, 2013), and subjected to a pushover analysis. A constant axial load ratio $v_d=0.15$ and two different reinforcement layouts (Figure 4a) were considered: one representing a concentrated reinforcement layout with boundary elements, the other standing for a distributed reinforcement arrangement (Figure 4a). To make the comparison between the analyses meaningful, the amounts of reinforcement were chosen such that the two cases provide the same moment resistance at 2% drift (Figure 5a).

Figure 4b and Figure 4d display the crack patterns of the walls at a drift of 3%, which was considered as the limit for the numerical reliability of the present analyses. It is evident that in case of concentrated reinforcement layout the crack widths in the boundary zones are relatively small when compared to the web region. For the distributed layout, the cracks are more uniform along the wall length and there is no sudden change in crack width between the confined boundary zones and the web region of the wall. The cracks in the lightly reinforced web of the wall with the concentrated reinforcement layout are much wider than the crack widths in the web of the wall with the distributed reinforcement layout, as depicted in Figure 5b. Lastly, it is noted that the distinct reinforcement layouts also influence the wall failure mechanism: due to large crack widths in the web, the concentrated layout led to premature sliding shear failure at the base of the wall according to (Figure 4c), while for the distributed layout the crack widths are better controlled and the wall failed due to crushing of the compressed zone (Figure 4e).

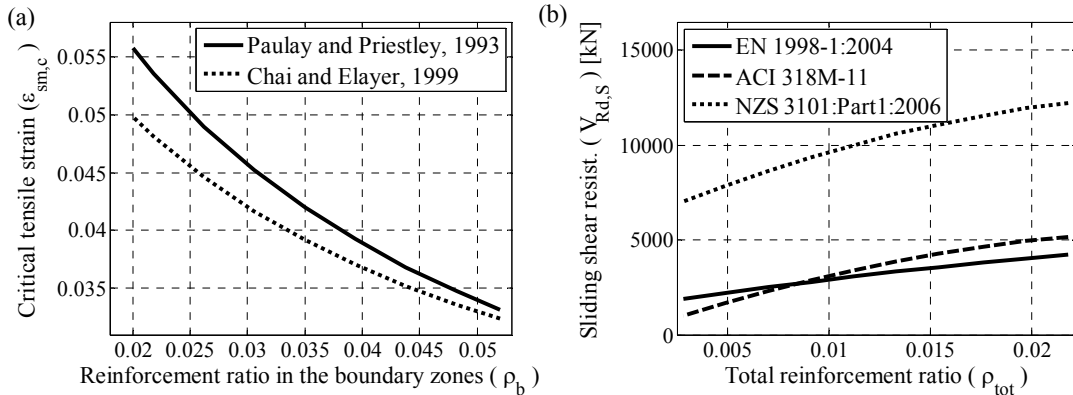


Figure 3. (a) Maximum tensile strain as a function of the reinforcement ratio in the boundary zone; (b) Design shear resistance against sliding as a function of the total reinforcement ratio in the critical section in which sliding shear failure may occur.

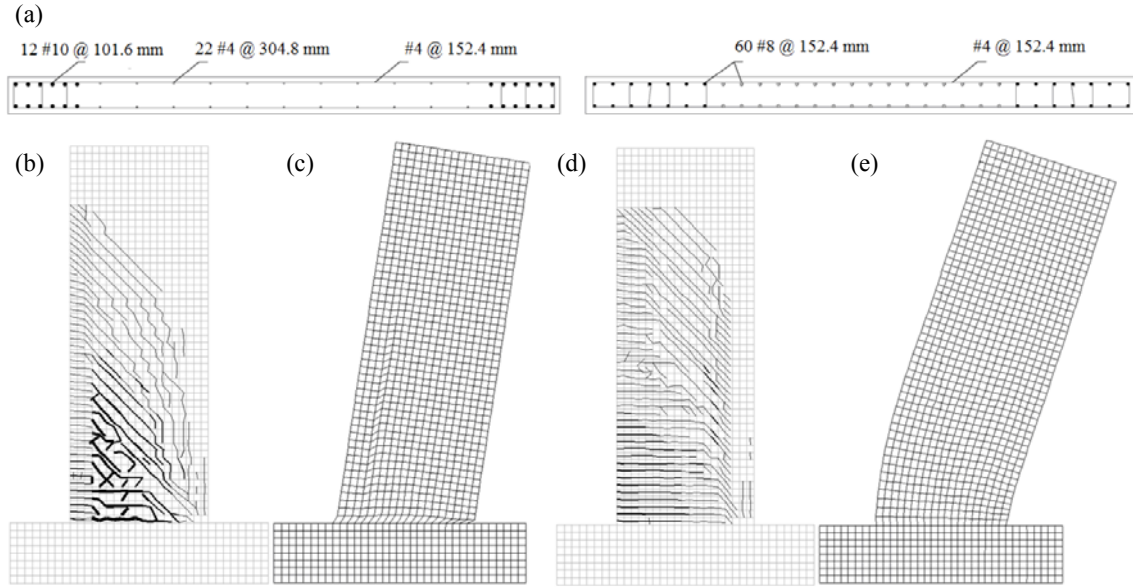


Figure 4. (a) Reinforcement layouts at the wall base; (b) Crack pattern at 3% drift for the concentrated reinforcement layout; (c) Sliding shear failure mechanism at the base for the concentrated reinforcement layout; (d) Crack pattern at 3% for the distributed reinforcement layout; (e) Crushing of the compressed zone for the distributed reinforcement layout.

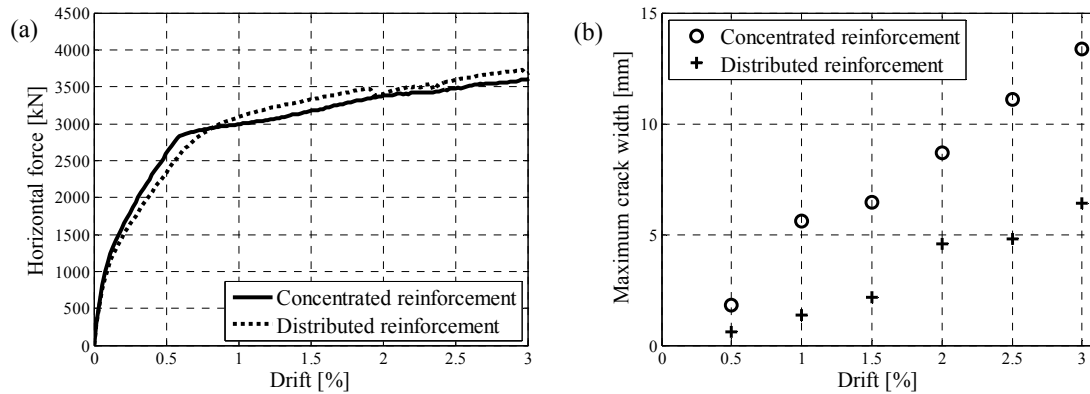


Figure 5. (a) Wall pushover results until 3% drift; (b) Estimates of maximum crack width.

CONCLUSIONS

In this paper, the influence of concentrated and distributed longitudinal reinforcement layouts on the lateral load response of rectangular RC walls has been investigated. Several different issues that affect the wall response were examined using available models, code recommendations and nonlinear monotonic analyses with shell elements. It was found that commonly used wall details with concentrated reinforcement at the wall ends can cause undesirable response with respect to the following points:

- Buckling of boundary zones: for boundary elements with concentrated reinforcement, instability may occur at a reduced eccentricity, causing wall out-of-plane failure at lower drift levels.
- Shear sliding failure: lower amounts of reinforcement used in the web region when walls are designed with a concentrated reinforcement layout cause wider cracks in this region, making the walls to experience shear sliding due to reduction in shear resistance at the crack interface.

With distributed reinforcement layouts, the compression zones will be longer than those obtained for concentrated reinforcement layouts. As a result, somewhat larger wall area needs to be confined. The confining reinforcement ratio required in the boundary zones according to all three codes considered in this study (Eurocode 8, ACI 318 and NZS 3101) increases with increasing longitudinal reinforcement ratio. The relations proposed in ACI 318 and NZS 3101 to compute the reinforcement content are applicable for any layout, while the one suggested in Eurocode 8 provides unreasonably high values in case of distributed layouts. For this reason, a modified expression was derived, which is suitable for concentrated and distributed reinforcement layouts (Eq. (30)).

Numerical analyses of walls suggested additional benefits of distributing the longitudinal reinforcement, which include more uniform flexural crack pattern, smaller crack widths, and more likelihood of eliminating brittle failure mechanisms.

In consideration of all of the aforementioned points, it is concluded that distributing a significant portion of the longitudinal reinforcement in walls with appropriate confinement reinforcement in the boundary zones will produce more dependable ductile wall response than that expected for comparable walls with concentrated reinforcement layouts as used in current design practice.

REFERENCES

- ACI Committee 318 (2011) "Building Code Requirements for Structural Concrete and Commentary" (ACI 318M-11), American Concrete Institute, Farmington Hills, MI.
- Beyer K, Dazio A, Priestley MJN. (2008) "Quasi-static cyclic tests of two U-shaped reinforced concrete walls", *Journal of Earthquake Engineering* 12, 1023-1053.
- Brueggen BL. (2009) Performance of T-Shaped Reinforced Concrete Structural Walls Under Multi-Directional Loading, Ph.D. Thesis, University of Minnesota, Twin Cities, MN, 499 pp.
- CEN (2004) "Eurocode 8: Design of structures for earthquake resistance, Part 1: General rules, seismic actions and rules for buildings" (EN 1998-1:2004), European Committee for Standardisation, Brussels, Belgium.
- Chai, Y.H. and Elayer, D.T. (1999) "Lateral Stability of Reinforced Concrete Columns under Axial Reversed Cyclic Tension and Compression", *ACI Structural Journal* 96 (5) 780-789.
- Chai, Y.H. and Kunnath, S.K. (2005) "Minimum thickness for ductile RC structural walls", *Engineering Structures* 27 (7) 1052-1063.
- Fardis, M.N. (2009) Seismic Design, Assessment and retrofitting of concrete buildings, 1st Ed., Springer.
- Moehle, J.P. (1992) "Displacement based design of RC structures", *Earthquake Spectra* 8 (3) 403-428.
- New Zealand Standard (2006) "Concrete Structures Standard. Part 1 – The Design Concrete Structures" (NZS 3101 Part 1:2006), Standards Association of New Zealand, Wellington, New Zealand.
- Paulay, T. and Priestley, M.J.N. (1992) Seismic Design of Reinforced Concrete and Masonry Buildings, John Wiley & Sons, Inc.
- Paulay, T. and Priestley, M.J.N. (1993) "Stability of Ductile Structural Walls", *ACI Structural Journal* 90 (4) 385-392.
- Preti M. and Giuriani E. (2011) "Ductility of a Structural Wall with Spread Rebars Tested in Full Scale", *Journal of Earthquake Engineering* 15, 1238-1259.
- Priestley, M.J.N. (2003) "Myths and Fallacies in Earthquake Engineering, revisited", *The Mallet Milne Lecture*, IUSS Press, Pavia, Italy.
- Salonikios, T.N., Kappos, A.J., Tegos, I.A., Penelis, G.G. (2000) "Cyclic Load Behaviour of Low-Slenderness Reinforced Concrete Walls: Failure Modes, Strength and Deformation Analysis, and Design Implications", *ACI Structural Journal* 97 (1) 132-141.
- Sritharan S, Beyer K, Henry RS, Chai YH, Kowalsky M, Bull D. (2014) "Understanding Poor Seismic Performance of Concrete Walls and Design Implications", *Earthquake Spectra*, In-Press.
- Wong, P. and Vecchio, F.J. (2013). *VecTor2 and Formworks Manual*. University of Toronto, Department of Civil Engineering, Canada.